Angular dependent time delay near correlation induced Cooper minima

Anatoli S. Kheifets[1]

[1]Research School of Physics, The Australian National University, Canberra ACT 0200, Australia

Daniele Toffoli[2] **and Piero Decleva**[2,3]

[2]Dipartimento di Scienze Chimiche e Farmaceutiche, Università degli Studi di Trieste, Trieste, Italy
[3]CNR-IOM DEMOCRITOS, Trieste, Italy

Abstract. We analyze an angular dependence of the Wigner time delay near the Cooper minimum (CM) of the sub-valent ns shell in argon, krypton and xenon. Such an angular dependence is a result of interplay between the relativistic and correlation effects. The correlation with the outermost np valence shell induces a CM in the sub-valent ns shell which is otherwise a CM free. A phase difference between the two spin-orbit split ionization continua $Ep_{1/2}$ and $Ep_{3/2}$ makes the Wigner time delay angular dependent. Both these effects are accounted for within a relativistic formulation of the random phase approximation (RRPA) and the time-dependent density functional theory (RTDDFT). Comparison between these two approaches illustrates a very strong sensitivity of the observed effect to the computation detail, especially the account of the ground state correlation.

PACS numbers: 32.80.Rm, 32.80.Fb, 42.50.Hz

1. Introduction

An electron group delay in a dispersive potential relative to the free space propagation, also known as the Wigner time delay, has been introduced to characterize a time-resolved electron scattering (Wigner 1955). A similar definition has been adopted in time-resolved photoionization where the Wigner time delay is defined as the energy derivative of the whole phase of the photoionization amplitude. The latter may include several competing and interacting channels (Pazourek *et al* 2015). With this extended definition, the Wigner time delay has become a subject of intense investigation following the pioneering experiments (Schultze *et al* 2010, Klünder *et al* 2011). These and the subsequent measurements (Guénot *et al* 2012, Guénot *et al* 2014, Palatchi *et al* 2014, Isinger *et al* 2017, Jain, Gaumnitz, Kheifets and Wörner 2018, Jain, Gaumnitz, Bray, Kheifets and Wörner 2018, Hammerland *et al* 2019) concentrated on the valence shells of noble gas atoms. The photoelectron detection in these experiments was either indiscriminate with respect to the emission angle or selected the photoelectrons in the direction of the laser field polarization. In more refined experiments (Heuser *et al* 2016, Cirelli *et al* 2018), angular dependence of the Wigner time delay was also recorded. In He, the lightest noble gas atom, the angular dependence of the time delay is caused solely by the probing field of the two-photon pump-probe measurement. Indeed, the Wigner time delay in the primary ionization channel $1s \to Ep$ is expressed via the energy derivative of the corresponding phase shift $\tau_{\rm W} = d\delta_p(E)/dE$ and thus carries no angular dependence. The probing field splits the Ep continuum into the two competing channels $E's$ and $E'd$, each supported by its own spherical harmonics. This makes the measured atomic time delay $\tau_a = \tau_{\rm W} + \tau_{\rm CC}$ angular dependent. Here $\tau_{\rm CC}$ is the continuum-continuum correction introduced by the probing field (Dahlström *et al* 2012) and it is this rather universal correction that carries the angular dependence. In heavier noble gases with the np valence shell, the Wigner time delay itself becomes angular dependent due to competition of the two primary ionization continua Es and Ed (Ivanov and Kheifets 2017). This competition becomes particularly intense near a Cooper minimum of the stronger ionization channel $np \to Ed$ (Bray *et al* 2018) or a Fano resonance due to a discrete excitation in the sub-valent ns shell (Cirelli *et al* 2018). In both cases, the angular dependence of the Wigner time delay becomes especially strong.

In the present work, we analyze yet another physical situation when the Wigner time delay becomes angular dependent. This is the case of a correlation induced Cooper minimum in the sub-valent ns shell of noble gas atoms: Ar $3s$, Kr $4s$ and Xe $5s$. Conventionally, the Cooper minimum (CM) in the valence shells of noble gas atoms is attributed to the sign change of the radial overlap of the bound np and continuous Ed orbitals. The origin of the CM in the sub-valent ns shells is more complex. It is induced by inter-shell correlation with the neighbouring np shell which passes through its own kinematic CM. This type correlation is very well documented. It can be accounted for by various theoretical approaches such as the random phase approximation with exchange (RPAE) (Amusia 1990) and its relativistic implementation (RRPA) (Johnson and Lin

1979), the multi-channel multi-configuration Dirac-Fock method (MMCDF) (Tulkki 1993), the relativistic time-dependent density functional theory (RTDDFT) (Toffoli *et al* 2002*a*) and, most recently, by the multi-configuration Tamm-Dankoff (MCTD) method (Aarthi *et al* 2014). In the relativistic formulation, photoionization of the ns shell leads to the two spin-orbit split continua $Ep_{1/2}$ and $Ep_{3/2}$, each of which is supported by its own scattering phase and the spherical harmonic. When the scattering phases differ substantially, this difference leads to a noticeable angular dependence of the time delay. We demonstrate such a situation near the CM where the scattering phases in both ionization channels undergo a shift of one unit of π. In the progression of atoms from Ar to Xe, this phase shift becomes noticeably separated between the $Ep_{1/2}$ and $Ep_{3/2}$ continua resulting in increasingly strong angular dependence of $\tau_{\rm W}$.

In the present work, we describe this effect by the two complimentary techniques, the RRPA and RTDDFT. The RRPA has been implemented recently for Wigner time delaty claculations in noble gas atoms (Saha *et al* 2014, Kheifets *et al* 2016, Keating *et al* 2018) and their isolelectronic ions (Saha, Deshmukh, Kheifets and Manson 2019, Saha, Jose, Deshmukh, Aravind, Dolmatov, Kheifets and Manson 2019) The RTDDFT has never been employed previously in this context. Both techniques account for the same physical processes by mixing the one-electron-one-hole excitations in the final ionized state. The difference is in treating the exchange between the electron-hole pairs. In the RRPA it is included explicitly into the exchange Coulomb matrix whereas in the TDDFT it is absorbed into the exchange-correlation functional. In addition, this functional takes into account the ground state correlation which is only partially included in RRPA by the so-called "time-reverse" diagrams ending with the photon interaction (Amusia 1990).

Extensive presentation of the RTDDFT formalism is given by Toffoli *et al* (2002*a*). In brief, the (relativistic) TDDFT approach is formally very close to RPAE. It includes the linear response of the electronic cloud to the external perturbing field. However, instead of starting from the Hartree-Fock reference, it employs the Kohn-Sham orbitals and density, which is obtained substituting the exchange term in HF with the exchange-correlation potential $V_{\rm XC}(\rho)$ of the density functional theory, which includes some correlation contribution. Also, in the response kernel, the exchange contribution is substituted by the first order change in $V_{\rm XC}$. So the correlation built into $V_{\rm XC}$ affects both the single particle orbitals and energies, and the strength of the coupling between different channels. As will be shown below, the latter may contribute to the much reduced Cooper minimum strength in the valence ns shell.

The paper is organized as follows. In Sec. 2 we outline relativistic formulation of the Wigner time delay and describe our computational implementation of the RRPA and RTDDFT methods. In Sec. 3 we present our numerical results for the photoionization cross-section, angular anisotropy β parameter and the Wigner time delay $\tau_{\rm W}$. We conclude in Sec. 4 by relating our findings with a possible experimental verification.

2. Formalism

We follow the derivation of our previous work (Kheifets *et al* 2016) where the angular dependence of the Wigner time delay in the np shell was analyzed. In this formalism, the electric dipole photoionization amplitude $T_{10}^{(1)}$ is evaluated by expansion over the spherical spinors with the spin $\nu = \pm\frac{1}{2}$ and angular momentum $\mu = \pm\frac{1}{2}$ projections. By adapting this formalism to the present case, we can write the photoionization amplitudes in the two spin-orbit split channels from a bound $ns_{1/2}$ state:

$$
\begin{aligned}
[T_{10}^{1+}]_{ns_{1/2}}^{m=\frac{1}{2}} &= \frac{-1}{3\sqrt{2}} Y_{10} D_{ns_{1/2}\to Ep_{1/2}} - \frac{1}{3} Y_{10} D_{ns_{1/2}\to Ep_{3/2}} \\
[T_{10}^{1-}]_{ns_{1/2}}^{m=\frac{1}{2}} &= \frac{1}{3} Y_{11} D_{ns_{1/2}\to Ep_{1/2}} - \frac{1}{3\sqrt{2}} Y_{11} D_{ns_{1/2}\to Ep_{3/2}}
\end{aligned}
\tag{1}
$$

For brevity of notations, we use a shortcut $[T_{10}^{1\pm}] \equiv [T_{10}^{1\mu=\pm\frac{1}{2}}]$. Here and throughout the text, $Y_{lm} \equiv Y_{lm}(\hat{\boldsymbol{k}})$ is the spherical harmonic evaluated in the direction of the photoelectron emission. The quantization direction $\hat{z}$ is chosen along the polarization axis. We also introduced the reduced matrix element modified by the phase factors:

$$
D_{lj\to\bar{l}\bar{j}} = i^{1-\bar{l}} e^{i\delta_{\bar{\kappa}}} \left\langle \bar{a} \| Q_J^{(\lambda)} \| a \right\rangle \tag{2}
$$

This reduced matrix element between the initial state $a = (n\kappa)$ and a final energy scale normalized state $a = (E, \bar{\kappa})$ is written as

$$
\left\langle \bar{a} \| Q_J^{(\lambda)} \| a \right\rangle = (-1)^{j+1/2} [\bar{j}][j] \begin{pmatrix} j & \bar{j} & J \\ -1/2 & 1/2 & 0 \end{pmatrix} \pi(\bar{l}, l, J-\lambda+1) R_J^{(\lambda)}(\bar{a}, a) \tag{3}
$$

Here $\pi(\bar{l}, l, J-\lambda+1) = 1$ or 0 for $\bar{l} + l + J - \lambda + 1$ even or odd, respectively, and $R_J^{(\lambda)}(\bar{a}, a)$ is the radial integral.

The signs $\pm$ in Equation (1) indicate the spin projections $\nu = \pm 1/2$ while $m = 1/2$ indicates the angular momentum projection. The analogous amplitudes with the $m = -1/2$ projection will have a similar structure with the simultaneous inversion of the spin projection $T^+ \leftrightarrow T^-$ and the second index of the spherical harmonic $Y_{21} \to Y_{2-1}$. Each amplitude has its own associated photoelectron group delay (Wigner time delay) defined as

$$
\tau_{\rm W} = \frac{d\eta}{dE} \quad , \quad \eta = \tan^{-1}\left[\frac{{\rm Im} T_{10}^{1\pm}}{{\rm Re} T_{10}^{1\pm}}\right] \ . \tag{4}
$$

The spin averaged time delay can be expressed as a weighted sum

$$
\bar{\tau}_{ns_{1/2}} = \frac{\tau_{ns_{1/2}}^{m=\frac{1}{2},+} \left| [T_{10}^{1+}]_{ns_{1/2}}^{m=\frac{1}{2}} \right|^2 + \left| [T_{10}^{1-}]_{ns_{1/2}}^{m=\frac{1}{2}} \right|^2 \tau_{ns_{1/2}}^{m=\frac{1}{2},-}}{\left| [T_{10}^{1+}]_{ns_{1/2}}^{m=\frac{1}{2}} \right|^2 + \left| [T_{10}^{1-}]_{ns_{1/2}}^{m=\frac{1}{2}} \right|^2} \tag{5}
$$

The angular momentum projection inversion $m = 1/2 \to m = -1/2$ does not affect this expression because of the axial symmetry of the photoionization process by linearly polarized laser field.

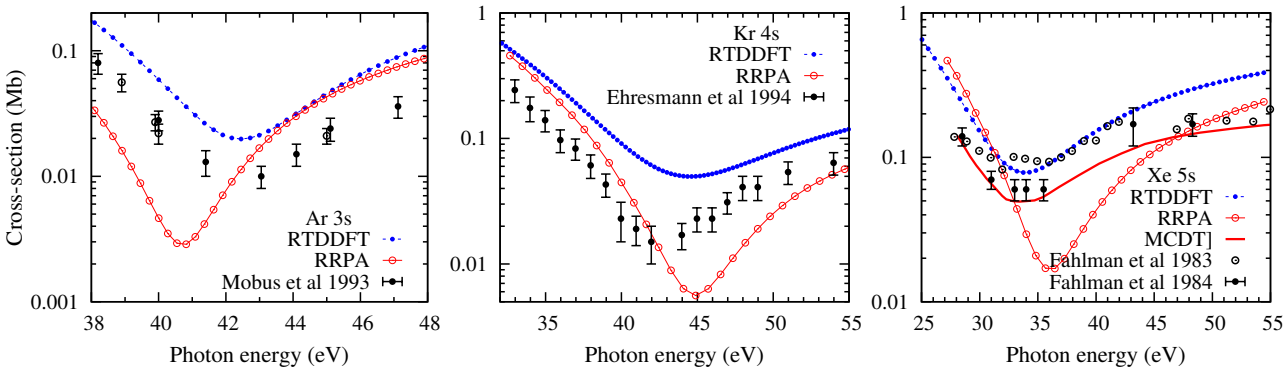

Figure 1. Photoionization cross-section in the region of the Cooper minima of Ar (left), Kr (center) and Xe (right). Comparison is made with experimental data for Ar (Möbus *et al* 1993), Kr (Ehresmann *et al* 1994) and Xe (Fahlman *et al* 1983, Fahlman *et al* 1984). For Xe, the MCTD calculation (Aarthi *et al* 2014) is also presened.

Knowing the ionization amplitudes we can also evaluate the angular anisotropy β parameter expressed as (Amusia 1990)

$$\beta_{ns_{1/2}} = \frac{|D_{Ep_{3/2}}|^2 - 2\sqrt{2}\mathrm{Re}[D^*_{Ep_{3/2}} D_{Ep_{1/2}}]}{|D_{Ep_{3/2}}|^2 + |D_{Ep_{1/2}}|^2} \ , \tag{6}$$

and the total photoionization cross-section which has the following form in the length gauge of the electromagnetic interaction (Johnson and Lin 1979):

$$\sigma_{ns_{1/2}} = \frac{4\pi^2}{3}\alpha a_0^2 \omega \left[|D_{Ep_{3/2}}|^2 + |D_{Ep_{1/2}}|^2 \right] . \tag{7}$$

Here α is the fine structure constant, a_0 is the Bohr radius and ω is the photon frequency.

We note that in the non-relativistic limit

$$D_{ns_{1/2}\to Ep_{1/2}} = -\sqrt{\frac{2}{3}} R_{ns\to Ep} \quad , \quad D_{ns_{1/2}\to Ep_{3/2}} = -\frac{2}{\sqrt{3}} R_{ns\to Ep} \tag{8}$$

and the β parameter acquires a constant value of 2. So a deviation of β from this value is a clear relativistic effect. We also note that in the limit (8) the amplitude $[T_{10}^{1-}]^{m=\frac{1}{2}}_{ns_{1/2}}$ vanishes and the Wigner time delay becomes angular independent as it is supported by a single spherical harmonic Y_{10}.

3. Numerical results

Our RRPA calculations comprised the following 18 relativistic channels:

$$\begin{aligned}
ns_{1/2} &\to Ep_{1/2},\ Ep_{3/2} \\
np_{1/2} &\to Es_{1/2},\ Ed_{3/2} \\
np_{3/2} &\to Es_{1/2},\ Ed_{3/2},\ Ed_{5/2} \\
(n-1)d_{3/2} &\to Ep_{1/2},\ Ep_{3/2},\ Ef_{5/2} \\
(n-1)d_{5/2} &\to Ep_{3/2},\ Ef_{5/2},\ Ef_{7/2} \\
(n-1)p_{1/2} &\to Es_{1/2},\ Ed_{3/2} \\
(n-1)p_{3/2} &\to Es_{1/2},\ Ed_{3/2},\ Ed_{5/2} \ .
\end{aligned} \tag{9}$$

In the case of Ar, where the subvalent d-shell was absent, only 12 photoionization channels were included. As in our previous work (Kheifets *et al* 2016), we employed the RRPA computer code developed by Johnson and co-workers (Johnson and Lin 1979). The RTDDFT dipole matrix elements have been obtained with an atomic B-spline code (Toffoli *et al* 2002*a*, Toffoli *et al* 2002*b*), with all allowed dipole channels included. The B-spline basis set (de Boor 1978) is of order ten and defined on a radial grid constructed according to the prescription of Fischer and Parpia (1993), and extending up to 20.0 au. Both the RRPA and RTDDFT calculations employed the experimental threshold energies. This way we included implicitly some two-electron-two-hole excitations in the final ionized state which otherwise are outside the scope of the both models.

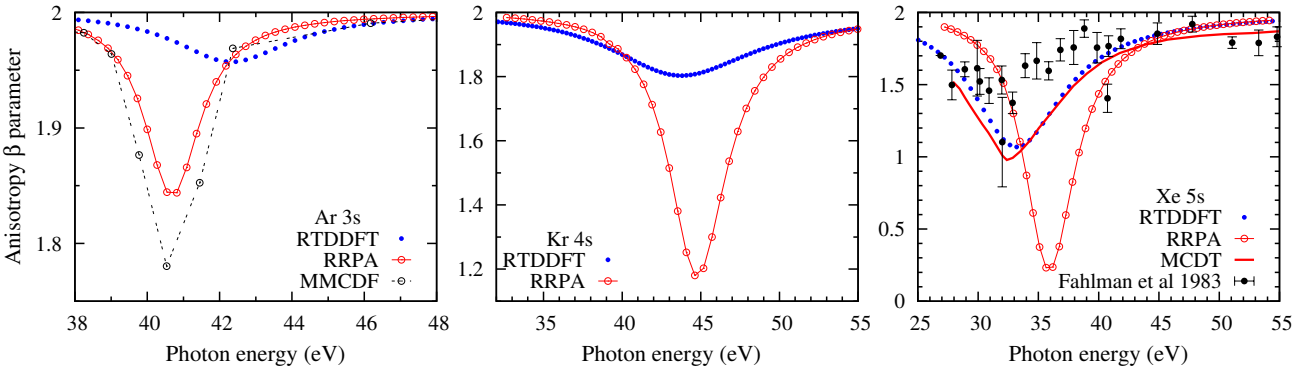

Figure 2. The angular anisotropy β parameters in the region of the Cooper minima of Ar (left), Kr (center) and Xe (right). On the left panel, the MMCDF calculation (Tulkki 1993) is shown. On the right panel, the MCTD calculation (Aarthi *et al* 2014) and the experimental data (Fahlman *et al* 1983) are also displayed.

First, we test our numerical results against the experimental values of the photoionization cross-sections for Ar (Möbus *et al* 1993), Kr (Ehresmann *et al* 1994) and Xe (Fahlman *et al* 1983, Fahlman *et al* 1984) as shown in Figure 1 (from left to right). The RRPA calculation always displays a deeper CM in comparison with RTDDFT. The experimental data are sandwiched in between the two calculations for Kr. For Ar and especially for Xe, they clearly favour RTDDFT.

In Figure 2 we show the calculated values of the anisotropy β parameters. We note that β deviates from its nonrelativistic value of 2 only near the Cooper minimum. This is particularly evident in the case of a lighter Ar atom where this deviation is very shallow. In heavier Kr and especially in the heaviest Xe, this deviation is very strong. In line with the cross-section results, the RRPA predicts a much deeper minima of the β-parameter near the CM. The experimental data (Fahlman *et al* 1983) clearly favour a more shallow RTDDFT β parameter.

This deficiency of the RRPA method near the CM, both for the cross-section and the β parameter, was noted by Fahlman *et al* (1983) very soon after RRPA photoionization parameters were tabulated by Huang *et al* (1981). However, the nature of this deficiency

has not been addressed and explained until recently. Aarthi *et al* (2014) suggested that this deficiency can be remedied by inclusion of (i) the ground state correlation and (ii) certain two-electron excitation and ionization channels. Indeed, the MCTD calculation for Xe (Aarthi *et al* 2014) is much closer to the experimental data (Fahlman *et al* 1983) than the RRPA, both for the cross-section and the β parameter (right panels of Figure 1 and figure 2, respectively). The RTDDFT technique does include the ground state correlation by way of the correlation and exchange functional. However, similarly to RRPA, it does not include any two-electron excitations. Hence, by making a comparison of MCDT and RTDDFT, which are very close near the CM, we may conclude that it is an unaccounted ground state correlation effect that largely causes deficiency of the RRPA. The inclusion of the two-electron excitations to MCDT make it closer to the experiment away from the CM. However, it causes a very strong gauge divergence of this method. The MCDT results shown in Figure 1 and 2 are in the length gauge of the electromagnetic interaction. The corresponding velocity gauge results (not shown) deviate from the experiment (Fahlman *et al* 1983) even stronger than RRPA with the β parameter for Xe reaching nearly -1 near the CM.

The strong effect of the ground state correlation on the ns photoionization near the Cooper minimum can be understood from the multi-configuration expansion presented in (Aarthi *et al* 2014) for Xe. This expansion contains excitations in the following generic form:

$$5p_{1/2}^{2-\nu}5p_{3/2}^{4-\mu}5d_{3/2}^{\nu}5d_{5/2}^{\mu} \quad , \ \nu,\mu = 0,2,4$$

As is seen from Equation (9), the $5d_{3/2}$ bound state can be ionized to both the $Ep_{1/2}$ and $Ep_{3/2}$ continua whereas the $5d_{5/2}$ state can only couple to the $Ep_{3/2}$ one. This shifts the balance between the two relativistic ionization channels and changes, most noticeably, the phase dependent quantities such as the angular anisotropy β parameter.

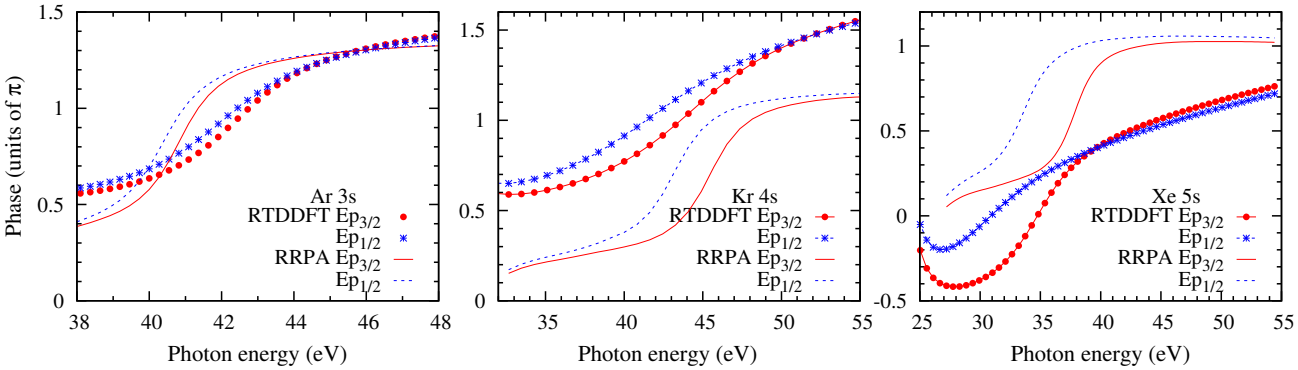

Figure 3. Phase variation of the ionization amplitudes $D_{Ep_{1/2}}$ and $D_{Ep_{3/2}}$ in the region of the Cooper minima of Ar (left), Kr (center) and Xe (right).

Because of a more complete account of the ground state correlation, we believe the accuracy of RTDDFT is superior to that of RRPA. In the following, we will give a stronger preference to the former over the latter. We will show the RRPA results only

for the sake of comparison and will use the RTDDFT calculations for making theoretical predictions for future experimental verification.

The evolution of the β parameter from Ar to Xe can be explained by the phase variation of the amplitudes $D_{Ep_{1/2}}$ and $D_{Ep_{3/2}}$ entering Equation (7) and illustrated in Figure 3. These amplitudes undergo a phase variation of one unit of π when passing through the CM. In argon, the lightest of the considered atoms, this phase variation is sharp and the phase deviation between the two spin-orbit split channels is small. When the energy derivative of the phase is taken, it is translated into a very large Wigner time delay which depends only weakly on the photoelectron emission angle as shown on the left panel of Figure 4. This is particularly true for the RTDDFT calculation in which β deviates from 2 only marginally. In heavier atoms, krypton and particularly xenon, the phase variation becomes more disperse. Consequently, the resulting time delay becomes smaller but more angular dependent at the same time. This angular dependence becomes particularly strong in Xe where a deviation of only 30° from the polarization direction results in a nearly 25% drop in the peak value of the time delay in the RRPA model. It is less so in RTDDFT where a noticeable variation of the time delay is observed at 60° relative to the polarization direction.

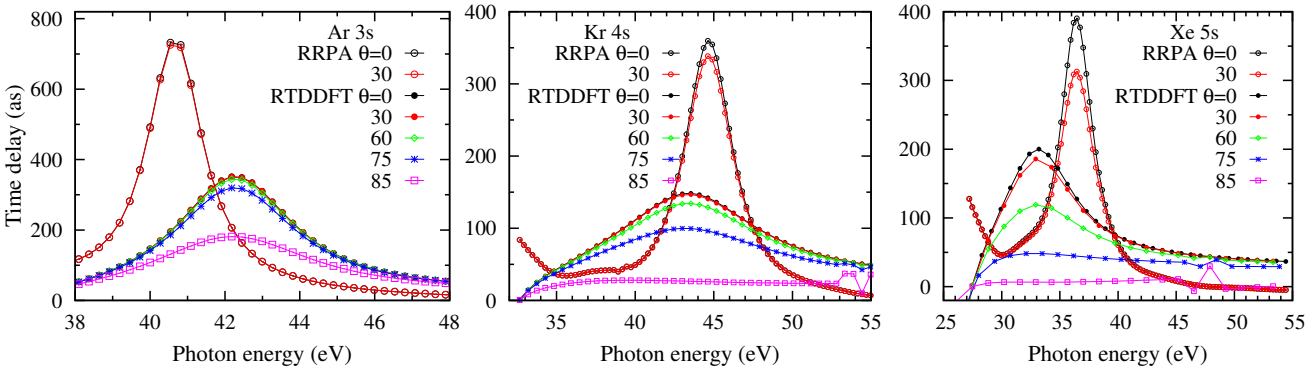

Figure 4. Angular variation of the Wigner time delay in the region of the Cooper minima of Ar (left), Kr (center) and Xe (right).

4. Discussion and outlook

Our numerical simulations indicate an angular dependence of the Wigner time delay in the region of the correlation induced Cooper minimum of noble gas atoms: Ar $3s$, Kr $4s$ and Xe $5s$. While this dependence is rather weak in the lightest argon atom, it is greatly enhanced in the heaviest target, xenon, where it can be readily measured experimentally.

The two aspects of this angular dependence should be highlighted. First, the Wigner time delay is only one component of the experimentally accessible atomic time delay $\tau_a = \tau_{\rm W} + \tau_{\rm CC}$. The latter is affected by the measurement induced CC-correction $\tau_{\rm CC}$ which is also angular dependent. For an ns target, this angular dependence stems

from the competition of the two ionization continua Es and Ed (Heuser *et al* 2016). This competition is particularly strong after the Ed partial wave goes through its kinematic node at the magic angle $\theta_m = 54.7°$. In result, the angular dependence of the atomic time delay in He becomes only noticeable above 60° detection angle. At a lesser deviation from the polarization direction, the atomic time delay in He is essentially flat. We expect that the same angular dependence of $\tau_{\rm CC}$ will be introduced into the atomic time delay measured in the ns shells of other noble gases. In Ar, the angular dependence of $\tau_{\rm CC}$ and $\tau_{\rm W}$ is comparable. The latter deviates noticeably from the polarization direction only at the emission angles as large as 60°. In krypton, this deviation becomes noticeable already at the emission angle as small as 30°. In xenon, at the emission angle of 30°, the Wigner component of the atomic time delay looses nearly 25% of its value whereas at 60° it retains less than one third of it. This makes the experimental observation of the angular dependent time delay in Xe plausible.

The second aspect of the present work that needs to be discussed is a persistent disagreement of the measured atomic time delay difference between the $3s$ and $3p$ shells of Ar. The initial experiments (Klünder *et al* 2011, Guénot *et al* 2012) were found in disagreement with predictions of the RPAE theory (Kheifets 2013) while the most recent measurement (Hammerland *et al* 2019) seems to show some closer agreement. Yet another latest report (Lejman *et al* 2019) states the disagreement with theory (Dahlström and Lindroth 2014) again. The measurement of Hammerland *et al* (2019) stands out from other experiments because the photoelectron emission was confined to the polarization direction. Other results were taken with the angular integration over all the possible emission directions. This, in principle, could affect the agreement with the calculation (Kheifets 2013) which was conducted in the polarization direction. However, based on our present evaluations, the angular dependence of the Wigner time delay near the $3s$ Cooper minimum in argon is too weak to explain this difference. Most recently, Hammerland (2019) suggested that the shake-up satellites of the $3p$ shell may fall into the region of the $3s$ Cooper minimum and thus complicate the analysis of the experimental data.

In conclusion, the authors wish to thank Hans Jakob Wörner who pointed their attention to the phenomenon investigated in the present work.

Aarthi G, Jose J, Deshmukh S, Radojevic V, Deshmukh P C and Manson S T 2014 Photoionization study of Xe 5s: ionization cross sections and photoelectron angular distributions *J. Phys. B* **47**(2), 025004

Amusia M Y 1990 *Atomic photoeffect* Plenum Press New York

Bray A W, Naseem F and Kheifets A S 2018 Simulation of angular-resolved RABBITT measurements in noble-gas atoms *Phys. Rev. A* **97**, 063404

Cirelli C, Marante C, Heuser S, Petersson C L M, Galán A J, Argenti L, Zhong S, Busto D, Isinger M, Nandi S, Maclot S, Rading L, Johnsson P, Gisselbrecht M, Lucchini M, Gallmann L and Dahlstr 2018 Anisotropic photoemission time delays close to a Fano resonance *Nature Comm.* **9**, 955

Dahlström J, Guénot D, Klünder K, Gisselbrecht M, Mauritsson J, Huillier A L, Maquet A and Ta¨eb R 2012 Theory of attosecond delays in laser-assisted photoionization *Chem. Phys.* **414**, 53–64

Dahlström J M and Lindroth E 2014 Study of attosecond delays using perturbation diagrams and exterior complex scaling *J. Phys. B* **47**(12), 124012

de Boor C 1978 *A Practical Guide to Splines* Springer, New York

Ehresmann A, Vollweiler F, Schmoranzer H, Sukhorukov V L, Lagutin B M, Petrov I D, Mentzel G and Schartner K H 1994 Photoionization of Kr 4*s*. III. Detailed and extended measurements of the Kr 4*s*-electron ionization cross section *J. Phys. B* **27**(8), 1489

Fahlman A, Carlson T A and Krause M O 1983 Angular distribution of xe $5s \rightarrow \epsilon p$ photoelectrons: Disagreement between experiment and theory *Phys. Rev. Lett.* **50**, 1114–1117

Fahlman A, Krause M O, Carlson T A and Svensson A 1984 Xe 5*s*, 5*p* correlation satellites in the region of strong interchannel interactions, 28-75 eV *Phys. Rev. A* **30**, 812–819

Fischer C F and Parpia F A 1993 Accurate spline solutions of the radial dirac equation *Physics Letters A* **179**(3), 198 – 204

Guénot D, Klünder K, Arnold C L, Kroon D, Dahlström J M, Miranda M, Fordell T, Gisselbrecht M, Johnsson P, Mauritsson J, Lindroth E, Maquet A, Ta¨eb R, L'Huillier A and Kheifets A S 2012 Photoemission-time-delay measurements and calculations close to the 3*s*-ionization-cross-section minimum in Ar *Phys. Rev. A* **85**, 053424

Guénot D, Kroon D, Balogh E, Larsen E W, Kotur M, Miranda M, Fordell T, Johnsson P, Mauritsson J, Gisselbrecht M, Varjù K, Arnold C L, Carette T, Kheifets A S, Lindroth E, L'Huillier A and Dahlström J M 2014 Measurements of relative photoemission time delays in noble gas atoms *J. Phys. B* **47**(24), 245602

Hammerland D 2019. private communication

Hammerland D, Zhang P, Bray A, Perry C F, Kuehn S, Jojart P, Seres I, Zuba V, Varallyay Z, Osvay K, Kheifets A, Luu T T and Woerner H J 2019 Effect of electron correlations on attosecond photoionization delays in the vicinity of the Cooper minima of argon *arXiv e-prints* p. arXiv:1907.01219

Heuser S, Jiménez Galán A, Cirelli C, Marante C, Sabbar M, Boge R, Lucchini M, Gallmann L, Ivanov I, Kheifets A S, Dahlström J M, Lindroth E, Argenti L, Mart´n F and Keller U 2016 Angular dependence of photoemission time delay in helium *Phys. Rev. A* **94**, 063409

Huang K N, Johnson W and Cheng K 1981 Theoretical photoionization parameters for the noble gases argon, krypton, and xenon *Atomic Data and Nuclear Data Tables* **26**(1), 33 – 45

Isinger M, Squibb R, Busto D, Zhong S, Harth A, Kroon D, Nandi S, Arnold C L, Miranda M, Dahlström J M, Lindroth E, Feifel R, Gisselbrecht M and L'Huillier A 2017 Photoionization in the time and frequency domain *Science* **358**, 893

Ivanov I A and Kheifets A S 2017 Angle-dependent time delay in two-color XUV+IR photoemission of He and Ne *Phys. Rev. A* **96**, 013408

Jain A, Gaumnitz T, Bray A, Kheifets A and Wörner H J 2018 Photoionization delays in xenon using single-shot referencing in the collinear back-focusing geometry *Opt. Lett.* **43**(18), 4510–4513

Jain A, Gaumnitz T, Kheifets A and Wörner H J 2018 Using a passively stable attosecond beamline for relative photoemission time delays at high XUV photon energies *Opt. Express* **26**(22), 28604–28620

Johnson W R and Lin C D 1979 Multichannel relativistic random-phase approximation for the photoionization of atoms *Phys. Rev. A* **20**, 964–977

Keating D A, Manson S T, Dolmatov V K, Mandal A, Deshmukh P C, Naseem F and Kheifets A S 2018 Intershell-correlation-induced time delay in atomic photoionization *Phys. Rev. A* **98**, 013420

Kheifets A, Mandal A, Deshmukh P C, Dolmatov V K, Keating D A and Manson S T 2016 Relativistic calculations of angle-dependent photoemission time delay *Phys. Rev. A* **94**, 013423

Kheifets A S 2013 Time delay in valence-shell photoionization of noble-gas atoms *Phys. Rev. A* **87**, 063404

Klünder *et al* K 2011 Probing single-photon ionization on the attosecond time scale *Phys. Rev. Lett.* **106**(14), 143002

Lejman M, Alexandridi C, Turconi M, Platzer L B D, Borot A, Hergott J F, Tcherbakoff O and Saliéres P 2019 Deauville, France pp. ID: 722 / TH–012

Möbus *et al* B 1993 Measurements of absolute Ar 3s photoionization cross sections *Phys. Rev. A* **47**(5), 3888–3893

Palatchi C, Dahlström J M, Kheifets A S, Ivanov I A, Canaday D M, Agostini P and DiMauro L F 2014 Atomic delay in helium, neon, argon and krypton *J. Phys. B* **47**(24), 245003

Pazourek R, Nagele S and Burgdörfer J 2015 Attosecond chronoscopy of photoemission *Rev. Mod. Phys.* **87**, 765

Saha S, Deshmukh P C, Kheifets A S and Manson S T 2019 Dominance of correlation and relativistic effects on photodetachment time delay well above threshold *Phys. Rev. A* **99**, 063413

Saha S, Jose J, Deshmukh P C, Aravind G, Dolmatov V K, Kheifets A S and Manson S T 2019 Wigner time delay in photodetachment *Phys. Rev. A* **99**, 043407

Saha S, Mandal A, Jose J, Varma H R, Deshmukh P C, Kheifets A S, Dolmatov V K and Manson S T 2014 Relativistic effects in photoionization time delay near the Cooper minimum of noble-gas atoms *Phys. Rev. A* **90**, 053406

Schultze *et al* M 2010 Delay in Photoemission *Science* **328**(5986), 1658–1662

Toffoli D, Stener M and Decleva P 2002*a* Application of the relativistic time-dependent density functional theory to the photoionization of xenon *J. Phys. B* **35**(5), 1275

Toffoli D, Stener M and Decleva P 2002*b* Photoionization of mercury: A relativistic time-dependent density-functional-theory approach *Phys. Rev. A* **66**, 012501

Tulkki J 1993 Combined effect of relaxation and channel interaction on outer-shell photoionization in Ar, K^+, and Ca^{2+} *Phys. Rev. A* **48**, 2048–2053

Wigner E P 1955 Lower limit for the energy derivative of the scattering phase shift *Phys. Rev.* **98**(1), 145–147